Effect of Co and Fe on the inverse magnetocaloric properties of Ni-Mn-Sn

Thorsten Krenke,[a] Eyüp Duman,[b] and Mehmet Acet[c]
Experimentalphysik, Universität Duisburg-Essen, D-47048 Duisburg, Germany

Xavier Moya, Lluís Mañosa, and Antoni Planes
Facultat de Física, Departament d'Estructura i Constituents de la Matèria, Universitat de Barcelona, Diagonal 647, E-08028 Barcelona, Catalonia, Spain

(Received 26 January 2007; accepted 15 June 2007; published online 2 August 2007)

At certain compositions Ni-Mn-*X* Heusler alloys (*X*: group IIIA–VA elements) undergo martensitic transformations, and many of them exhibit inverse magnetocaloric effects. In alloys where *X* is Sn, the isothermal entropy change is largest among the Heusler alloys, particularly in $Ni_{50}Mn_{37}Sn_{13}$, where it reaches a value of 20 J kg^{-1} K^{-1} for a field of 5 T. We substitute Ni with Fe and Co in this alloy, each in amounts of 1 and 3 at % to perturb the electronic concentration and examine the resulting changes in the magnetocaloric properties. Increasing both Fe and Co concentrations causes the martensitic transition temperature to decrease, whereby the substitution by Co at both compositions or substituting 1 at % Fe leads to a decrease in the magnetocaloric effect. On the other hand, the magnetocaloric effect in the alloy with 3 at % Fe leads to an increase in the value of the entropy change to about 30 J kg^{-1} K^{-1} at 5 T. © *2007 American Institute of Physics*.
[DOI: 10.1063/1.2761853]

I. INTRODUCTION

Since the observation of martensitic transformations in Ni-Mn based Heusler alloys,[1] and the later discovery of the magnetic shape memory effect (MSM) in Ni-Mn-Ga,[2] there has been growing interest in the magneto-mechanical properties of Ni-Mn-*X* systems (*X*: group IIIA–VA elements).[3–8] Martensitic transformations in these systems are found roughly in a valence electron concentration range of $7.4 \leq e/a \leq 8.5$ electrons per atom. Next to the MSM effect, large magnetocaloric effects (MCE) have been reported in the vicinity of the martensitic transformation in Ni-Mn-Ga (Ref. 9) and other Ni-Mn-based Heusler alloys such as Ni-Mn-Sn and Ni-Mn-In.[10–12] The MCE in these systems relies on the large and rapid temperature variation in the magnetic interaction around the martensitic transition. Furthermore, the MCE in Ni-Mn-based Heuslers is usually "inverse," i.e., the alloy cools on applying a magnetic field adiabatically instead of heating.[10] The magnitude of the inverse MCE is about 20 J kg^{-1} K^{-1} for 5 T in $Ni_{50}Mn_{37}Sn_{13}$ being comparable with those of giant MCE material.[13–15] The use of normal and inverse MCE materials in the form of composites can affect the heat transfer efficiency favorably in heating or cooling units based on the MCE.

To understand the influence of introducing small amounts of transition elements on the size of the MCE in $Ni_{50}Mn_{37}Sn_{13}$, we have investigated the entropy change around the martensitic transition of $(Ni,Co)_{50}Mn_{37}Sn_{13}$ and $(Ni,Fe)_{50}Mn_{37}Sn_{13}$, in which Ni was replaced by Fe and Co, each in amounts of 1 and 3 at %. Higher concentrations of Fe and Co lead nearly to the complete suppression of the martensitic state. The entropy change was determined from field-dependent magnetization measurements.

II. EXPERIMENT

Ingots of about 3 g were prepared by arc melting pure metals under argon atmosphere in a water-cooled Cu crucible. The ingots were then encapsulated under argon atmosphere in quartz glass and annealed at 1273 K for 2 h. Afterwards, they were quenched in ice water. The compositions of the alloys were determined by energy dispersive x-ray photoluminescence analysis (EDX) and are given in at % in Table I. The valence electron concentrations e/a are also given in the table. This is calculated as the concentration weighted sum of the number of 3*d* and 4*s* electrons of Ni and Mn and the number of 4*s* and 4*p* electrons of Sn. An estimated error of ±0.1% in determining the concentration leads to an error of ±0.007 in the value of e/a.

Polycrystalline samples were cut from the ingots using a low-speed diamond saw and used as samples for magnetization and calorimetric studies. For differential scanning calorimetry (DSC) measurements, one side of the samples was ground with 1200 grid SiC abrasive to ensure proper thermal

TABLE I. Compositions of the samples in at % determined by EDX analysis and the valence electron concentrations per atom e/a. The sample containing no Fe or Co is referred to as "Reference."

Sample	Ni	Co	Fe	Mn	Sn	e/a
Reference	49.9	···	···	37.1	13.0	8.107
Co1	48.7	1.2	···	36.9	13.2	8.089
Co3	47.0	3.1	···	36.6	13.3	8.073
Fe1	49.1	···	0.9	36.7	13.3	8.083
Fe3	46.9	···	3.0	36.8	13.3	8.038

[a]Present address: ThyssenKrupp Electrical Steel, F&E Ge, Kurt-Schumacher-Str. 95, D-45881 Gelsenkirchen, Germany.
[b]Present address: Heinrich Heine Universität Duesseldorf, Institut für Physik der kondensierten Materie, Abteilung für Materialwissenschaft, D-40225 Düsseldorf Germany.
[c]Electronic mail: macet@ttphysik-uni-duisburg.de

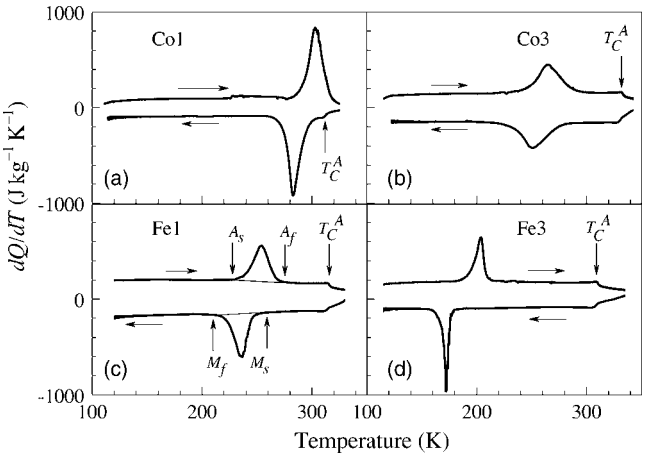

FIG. 1. dQ/dT vs temperature for the alloys undergoing martensitic transformations (a) Co1; (b) Co3; (c) Fe1; and (d) Fe3. Horizontal arrows indicate direction of temperature change. Vertical arrows in part (b) show as an example the positions of the martensitic and austenitic transition temperatures.

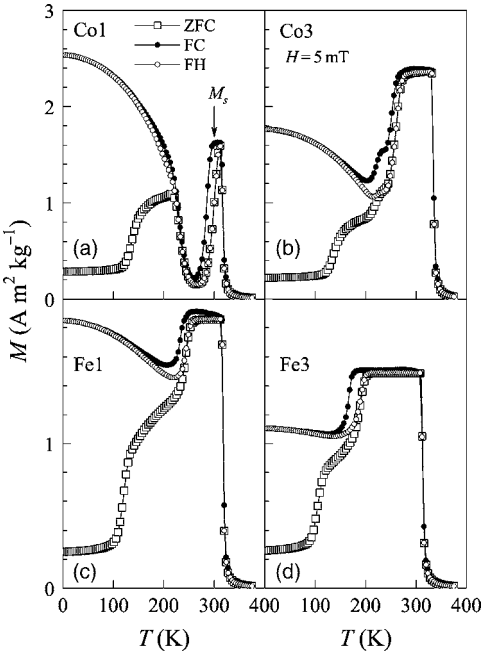

FIG. 2. ZFC, FC, and FH $M(T)$ in 5 mT of (a) Co1; (b) Co3; (c) Fe1; and (d) Fe3.

contact. Calorimetric measurements were carried out in the temperature range 100 K$\leq T\leq$350 K. Typical heating and cooling rates were 0.5 K min^{-1}.

The temperature dependence of the magnetization $M(T)$ was measured in magnetic fields $\mu_0 H$ of 5 mT and 5 T in the temperature range 5 K$\leq T\leq$380 K using a superconducting quantum interference device magnetometer. Prior to the measurements, the samples were prepared in a zero-field-cooled state (ZFC) by cooling it from 380 to 5 K in the absence of a magnetic field. Subsequently, an external field was applied, and the data were taken on increasing temperature up to 380 K. Then, without removing the external field, the data were taken on decreasing temperature, giving the field-cooled (FC) branch. As a last step, again without removing the external field, the magnetization was measured on increasing temperature. The last step is denoted as the field-heated (FH) sequence. Any hysteresis in the FC and FH sequences is expected to be associated with a structural transition, whereas any splitting of the ZFC and FH curves is expected to be associated with pinning due to antiferromagnetic (AF) or noncollinear magnetic structures existing within the ferromagnetic (FM) matrix. Such structures can reside within twin boundaries if the system is martensitic.

III. RESULTS AND DISCUSSION

A. Calorimetric studies

The results of the calorimetric experiments are collected in Fig. 1. Next to the features associated with the martensite start M_s, martensite finish M_f, austenite start A_s, and austenite finish A_f temperatures, features associated with the Curie temperature of the austenitic state T_C^A are also observed. For Co1, T_C^A is observed only in the cooling curve. In the heating curve, such a feature is masked by the intense peak associated with the reverse transition. The positions of T_C^A are in good agreement with those determined from the magnetization measurements (Sec. III B). The structural transition temperatures determined from the calorimetry data are indicated with a DSC subscript and are collected in Table II. Values for the reference sample $Ni_{50}Mn_{37}Sn_{13}$ from earlier data are also included in the table.[10] The transition temperatures decrease with respect to those of the reference sample as Fe or Co is substituted for Ni due to the decrease in the valence electron concentration.

B. Magnetization measurements

The temperature dependence of the FC, ZFC, and FH magnetization $M(T)$ measured in 5 mT is shown in Fig. 2. All samples order ferromagnetically in the austenitic state below T_C^A. With respect to T_C^A=311 K of the reference alloy, T_C^A increases with increasing Fe and Co concentrations, whereby the increase is more significant for the case of Co

TABLE II. Martensite start and finish temperatures (M_s,M_f), austenite start and finish temperatures (A_s,A_f) determined by DSC, and $M(T)$ measurements (DSC and M in superscript). T_C^A are also given. The reference sample containing no Fe or Co is labeled as "Ref."

Sample	M_s^{DSC} (K)	M_s^M (K)	M_f^{DSC} (K)	M_f^M (K)	A_s^{DSC} (K)	A_s^M (K)	A_f^{DSC} (K)	A_f^M (K)	T_C^A (K)
Ref	307	303	289	265	295	275	318	309	311
Co1	306	305	257	259	277	267	325	-	316
Co3	300	294	217	205	229	214	303	323	335
Fe1	259	261	209	208	228	221	279	280	316
Fe3	187	195	156	141	177	150	216	196	315

(Table II). For $T<T_C^A$, $M(T)$ is at the demagnetization limit in 5 mT and remains essentially temperature insensitive in all samples until it begins to drop at M_s. The M_s^M values given in Table II are taken as the temperature where the maximum in the FC-$M(T)$ data is observed. These values are in good agreement with M_s^{DSC}, whereby only the Fe3 sample has a larger difference in the values of M_s determined by the two methods. At lower temperatures, $M(T)$ runs through a minimum for all samples. The temperatures related to the minima lie somewhat lower than M_f determined from the DSC measurements. Similarly, A_s and A_f lie around the temperatures at which the FH-$M(T)$ curves exhibit a minimum and a maximum, respectively. Since any of these temperatures varies rapidly with composition, any major differences of the transition temperatures determined by the two methods can be related to small compositional differences in the samples used for the $M(T)$ and for the DSC experiments. In the case of the Co3 sample, an additional feature within the transition region is observed, which is indicative of an intermartensitic transition. However, the data are not conclusive, and further evidence is required to explain this feature.

The ZFC data in Fig. 2 begin at a low magnetization value of about 0.2 $\mathrm{Am^2\,kg^{-1}}$ due to the essentially random spatial configuration that the moments acquire while cooling through T_C down to low temperatures. At low temperatures, the spin system is in a frozen state. On heating, $M(T)$ remains constant up to about 100 K in all samples. At this temperature, the thermal energy begins to overcome the exchange anisotropy of the frozen state in the 5 mT measuring field, and the magnetization begins to increase. At a slightly higher temperature the rate of increase slows down, and eventually the ZFC and FH curves merge. This occurs at a temperature between A_s and A_f as the proportion of the austenitic phase increases, and along with it, ferromagnetic exchange gains strength.

$M(T)$ measured in 5 T is shown in Fig. 3. A difference in the ZFC and FH $M(T)$ curves no longer exists in this field, and ZFC data are omitted. However, a hysteresis is still present in the FC and FH curves for all samples. The hysteresis narrows with increasing Co content, while it becomes broader with increasing Fe content. The temperature corresponding to the peak in the FC-$M(T)$ curve shifts to lower values with respect to M_s found from the data in Fig. 2. The shift is about 10 K for the Co1 sample and 20–30 K for the other samples. For all samples, the magnetization drops as the structure transforms from austenite to martensite. This drop can be related to the fact that in Mn-based Heusler systems, the exchange interaction strongly depends on the Mn-Mn distance, and any change in the distance caused by a change in the crystal structure can modify the interactions and introduce antiferromagnetic exchange. This has been shown to be the case for a $Ni_{50}Mn_{36}Sn_{14}$ alloy, in which short-range antiferromagnetic exchange was found to be

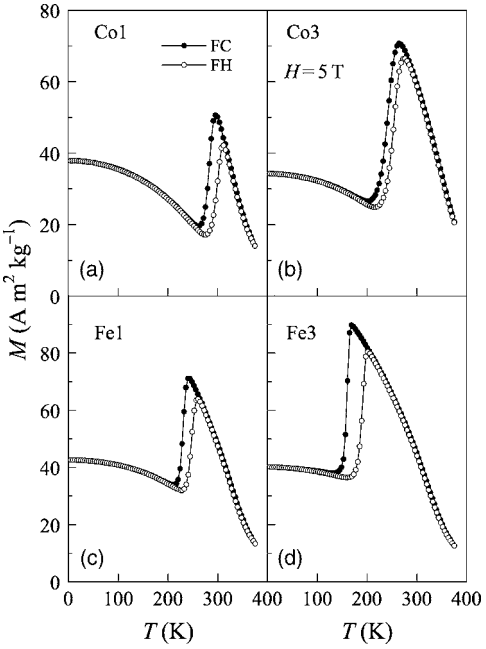

FIG. 3. (a) ZFC, FC, and FH $M(T)$ in 5 T of (a) Co1; (b) Co3; (c) Fe1; and (d) Fe3.

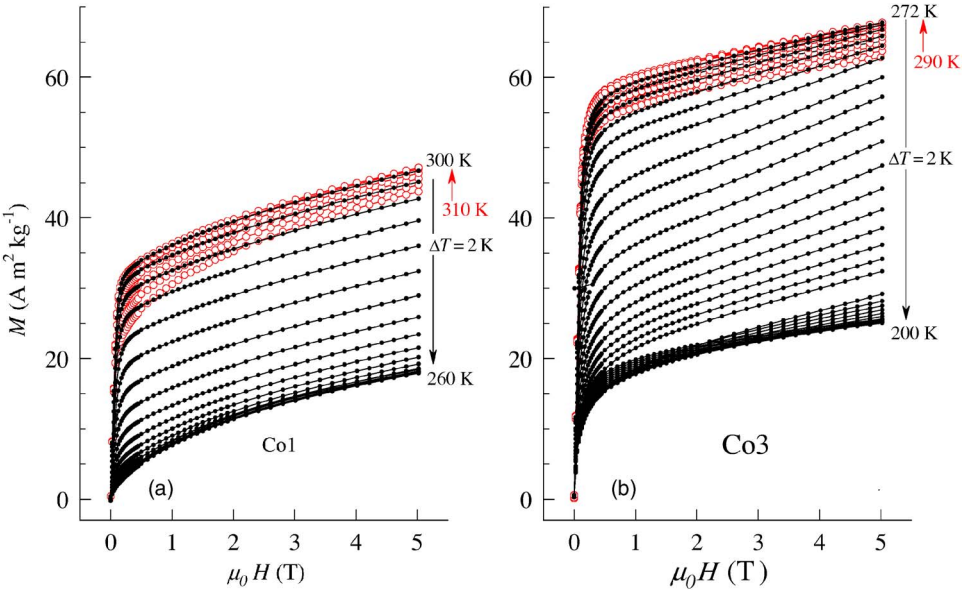

FIG. 4. (Color online) The field dependence of the magnetization for (a) Co1 and (b) Co3. The open circles refer to data for which the magnetization decreases from 300 to 310 K for Co1 and from 272 to 290 K for Co3. The vertical arrows indicate the temperature sequence of data collection.

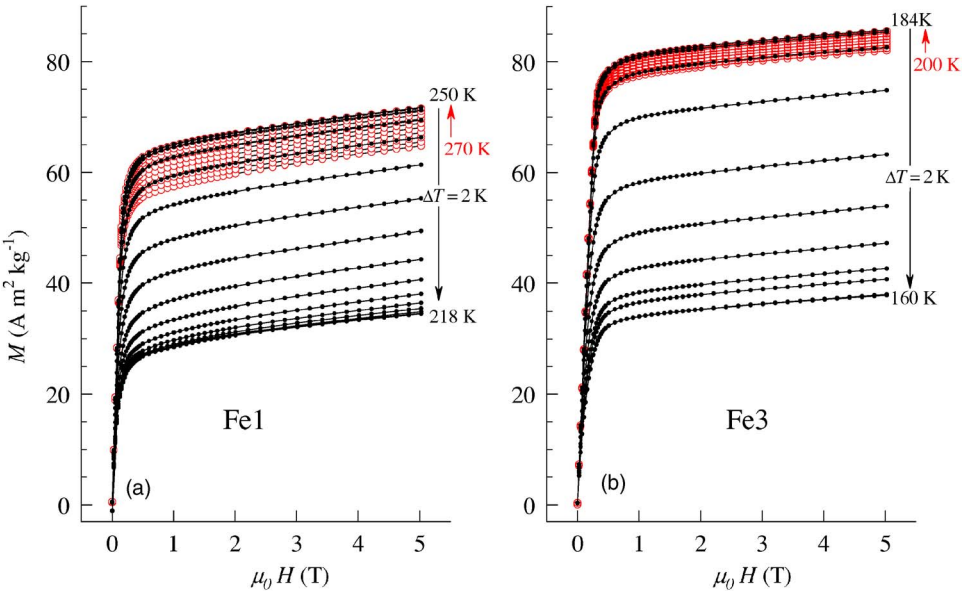

FIG. 5. (Color online) The field dependence of the magnetization for (a) Fe1 and (b) Fe3. The open circles (red) refer to data for which the magnetization decreases from 250 to 270 K for Fe1 and from 184 to 200 K for Fe3. The vertical arrows indicate the temperature sequence of data collection.

present between Mn atoms located at the 4(*b*) positions of the austenite phase and the exchange strengthens in the martensitic state.[16]

C. Magnetocaloric effects

To determine the size of the magnetocaloric effect (MCE) in the vicinity of the transition, we use the Maxwell relation

$$\Delta S(T,H) = \mu_0 \int_0^H \left(\frac{\partial M}{\partial T}\right)_H \mathrm{d}H, \tag{1}$$

from which the MCE can be estimated numerically from $M(H)$ isotherms. The $M(H)$ curves for the samples in the temperature range of their respective structural transition temperatures are given in Figs. 4 and 5. The curves are obtained on increasing field and decreasing temperature as indicated by the arrows. The sequence of measurements shown with open circles (red) shows an increase in $M(H)$ with decreasing temperature down to M_s for all samples. The behavior reverses below M_s. For Fe1, Fe3, and Co1, $M(H)$ increases steadily up to 5 T without any major feature. For Co3, there is a tendency for a metamagnetic-like transition for temperatures below M_s, as can be seen from the development of an upturn of the data with increasing field at an inflection point around 2–3 T. This feature is expected to be due to the onset of a field-induced transition from the martensitic to the austenitic state, which is the state of higher magnetization. The observability of this effect only in the Co3 sample is because the shift in M_s to lower temperatures in the applied fields in these experiments exceeds the width of the hysteresis in $M(T)$ (Fig. 2). For the other samples, the hysteresis is too broad to observe a field-induced transition up to 5 T.

The temperature dependencies of the entropy changes for the presently investigated samples are shown in Fig. 6. The addition of either Fe or Co causes e/a to decrease and, therefore, lowers the temperature corresponding to the peak position of ΔS. There is not much change in the value of ΔS when Co is alloyed. However, alloying 3 at % Fe leads to a marked increase up to 30 J kg^{-1} K^{-1} in ΔS for a field of 5 T with respect to the value of 20 J kg^{-1} K^{-1} for the nonalloyed sample.[10] This increase is evidently related to a comparatively large $\partial M/\partial T$ which would lead to a large ΔS through Eq. (1). For this particular concentration, a large $\partial M/\partial T$ can be found to lie in the large spacing of the magnetization isotherms in Fig. 5(b). Two additional peaks in ΔS appear for the Co3 sample around 240 and 260 K. These are expected to be related to the steplike features observed below M_s in the $M(T)$ data [Fig. 2(b)]. Such features can be associated with intermartensitic transformations, whereby the modulation of the martensite structure changes.

The maximum entropy change $\Delta S_{\max}$ obtained from Fig. 6 is plotted against the magnetic field in Fig. 7. In all cases, the variation of $\Delta S_{\max}$ with applied field is, to a good ap-

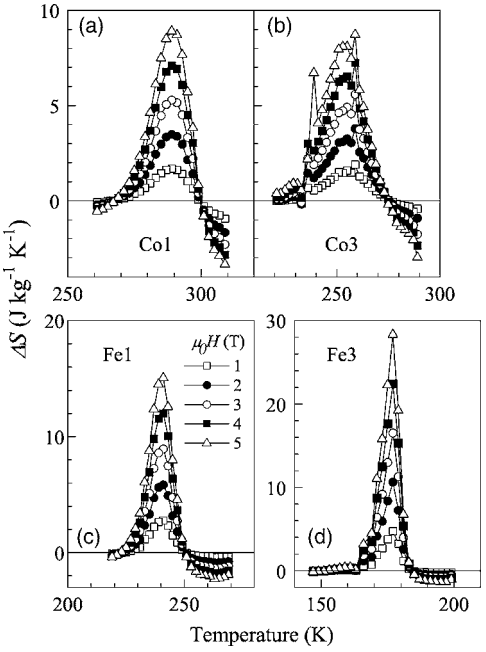

FIG. 6. The entropy change for (a) Co1; (b) Co2; (c) Fe1; and (d) Fe2.

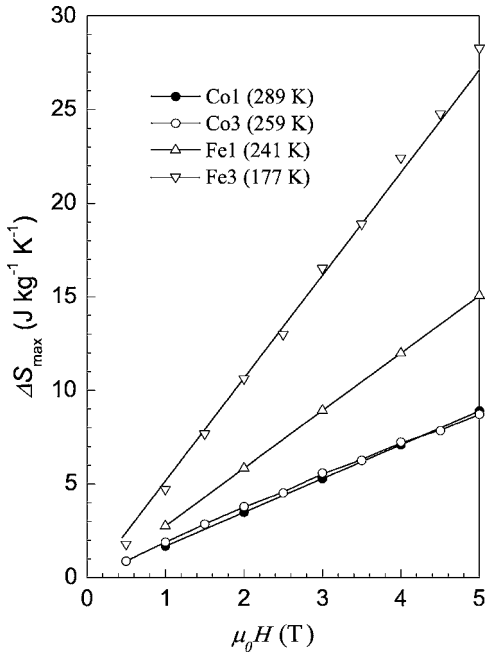

FIG. 7. The maximum in the entropy change as a function of applied field. The temperatures in the legend correspond to the positions of the maxima in ΔS in Fig. 6.

proximation, linear within the range of the experiments. The rate of increase of ΔS_{max} with field is 1.8 J kg^{-1} K^{-1} T^{-1} for Co1 and Co3; 3.0 J kg^{-1} K^{-1} T^{-1} for Fe1, and 5.5 J kg^{-1} K^{-1} T^{-1} for Fe3. There is no tendency to saturation for ΔS_{max} within the studied field range.

IV. CONCLUSION

We have studied the effects of varying the electron concentration by introducing small amounts of Fe and Co in place of Ni on the magnetocaloric effect of $Ni_{50}Mn_{37}Sn_{13}$. Introducing either of the elements leads to a decrease in M_s, whereby Co reduces ΔS, and 3 at % Fe leads to an increase in ΔS. The increase is related to the increase in $\partial M/\partial T$. The thermal hysteresis associated with the transition becomes narrower with Co substitution, whereas it broadens when Fe is added.

ACKNOWLEDGMENTS

We thank Peter Hinkel for technical support. This work was supported by Deutsche Forschungsgemeinschaft (GK277, SPP 1239) and CICyT (Spain), Project MAT2004-1291. X.M. acknowledges support from DGICyT (Spain).

[1] P. J. Webster, K. R. A. Ziebeck, S. L. Town, and M. S. Peak, Philos. Mag. B **49**, 295 (1984).
[2] K. Ullakko, J. K. Huang, C. Kantner, R. C. O'Handley, and V. V. Kokorin, Appl. Phys. Lett. **69**, 1966 (1996).
[3] M. Acet, E. Duman, E. F. Wassermann, L. Mañosa, and A. Planes, J. Appl. Phys. **92**, 3867 (2002).
[4] Y. Sutou, Y. Imano, N. Koeda, T. Omori, R. Kainuma, K. Ishida, and K. Oikawa, Appl. Phys. Lett. **85**, 4358 (2004).
[5] T. Krenke, M. Acet, E. F. Wassermann, X. Moya, L. Mañosa, and A. Planes, Phys. Rev. B **72**, 014412 (2005).
[6] T. Krenke, M. Acet, E. F. Wassermann, X. Moya, L. Mañosa, and A. Planes, Phys. Rev. B **73**, 174413 (2006).
[7] K. Oikawa, W. Ito, Y. Imano, Y. Sutou, R. Kainuma, K. Ishida, S. Okamoto, O. Kitakami, and T. Kanomata, Appl. Phys. Lett. **88**, 122507 (2006).
[8] K. Koyama, K. Watanabe, T. Kanomata, R. Kainuma, K. Oikawa, and K. Ishida, Appl. Phys. Lett. **88**, 132505 (2006).
[9] J. Marcos, L. Mañosa, A. Planes, F. Casanova, X. Batlle, A. Labarta, and B. Martínez, Phys. Rev. B **66**, 224413 (2002); J. Marcos, L. Mañosa, A. Planes, F. Casanova, X. Batlle, and A. Labarta, *ibid.* **68**, 094401 (2003).
[10] T. Krenke, M. Acet, E. F. Wassermann, X. Moya, L. Mañosa, and A. Planes, Nat. Mater. **4**, 450 (2005).
[11] Z. D. Han, D. H. Wang, C. L. Zhang, S. L. Tang, B. X. Gu, and Y. W. Du, Appl. Phys. Lett. **89**, 182507 (2006).
[12] T. Krenke, M. Acet, E. Duman, E. F. Wassermann, X. Moya, L. Mañosa, A. Planes, E. Suard, and B. Ouladdiaf, Phys. Rev. B **65**, 104414 (2007).
[13] V. K. Pecharsky and K. A. Gschneidner, Jr., J. Magn. Magn. Mater. **200**, 44 (1999).
[14] K. A. Gschneidner, Jr., V. K. Pecharsky, and A. O. Tsokol, Rep. Prog. Phys. **68**, 1479 (2005).
[15] E. Brück, J. Phys. D **38**, R381 (2005).
[16] P. J. Brown, A. P. Gandy, K. Ishida, R. Kainuma, T. Kanomata, K. U. Neumann, K. Oikawa, B. Ouladdiaf, and K. R. A. Ziebeck, J. Phys.: Condens. Matter **18**, 2249 (2006).